INSTITUTE OF PHYSICS PUBLISHING JOURNAL OF PHYSICS: CONDENSED MATTER

J. Phys.: Condens. Matter **15** (2003) 6943–6953 PII: S0953-8984(03)66322-8

Comparison between classical potentials and *ab initio* methods for silicon under large shear

J Godet, L Pizzagalli, S Brochard and P Beauchamp

Laboratoire de Métallurgie Physique, CNRS UMR 6630, Université de Poitiers, BP 30179, 86962 Futuroscope Chasseneuil Cedex, France

E-mail: Laurent.Pizzagalli@univ-poitiers.fr

Received 15 July 2003
Published 3 October 2003
Online at stacks.iop.org/JPhysCM/15/6943

Abstract

The homogeneous shear of the {111} planes along the ⟨110⟩ direction of bulk silicon has been investigated using *ab initio* techniques, to better understand the strain properties of both shuffle and glide set planes. Similar calculations have been done with three empirical potentials, Stillinger–Weber, Tersoff and EDIP, in order to find the one giving the best results under large shear strains. The generalized stacking fault energies have also been calculated with these potentials to complement this study. It turns out that the Stillinger–Weber potential better reproduces the *ab initio* results, for the smoothness and the amplitude of the energy variation as well as the localization of shear in the shuffle set.

(Some figures in this article are in colour only in the electronic version)

1. Introduction

Dislocations in materials generate a long-range strain field, which must be taken into account in atomistic simulations for a proper treatment of the defects. As a consequence, large systems including thousands of atoms have to be employed. Only in specific cases is it possible to use a limited number of atoms. For example, if the considered dislocations are ideally straight and infinite, the core structure may be investigated with a few hundred atoms. Precise electronic and atomic structure calculations can then be performed using *ab initio* methods [1–5]. Still, investigating the formation, mobility or interaction of dislocations requires a large system with a few thousand atoms [6], preventing the use of such methods. Then the atomic simulation must be performed with empirical interatomic potentials.

With such potentials, the simulations can be performed with a large number of atoms and for a long timescale, with a moderate cost in calculation time. Then, they are a valuable mean for simulating the activation of complex physical mechanisms, using techniques like molecular dynamics. However, it remains difficult to evaluate the validity of the results obtained from

such studies. Interatomic potentials are built in order to reproduce with a fair accuracy a limited number of physical quantities, usually at equilibrium. The reliability of potentials is then doubtful when one investigates physical mechanisms or configurations where the atomic structure is far from its equilibrium state, such as, for example, reconstruction of surfaces or point or extended defects. Moreover, the nature of the material is also an important factor. It is commonly agreed that the results obtained using interatomic potentials are qualitatively better for metals than in the case of covalent materials. This problem is very sensible for silicon in particular, since it is widely studied, for technology purposes, or as a model for semiconductors. Several kinds of potential have been proposed but it is difficult to assess the superiority of one over another. In particular, the transferability is poor in many cases. Several comparative studies on elastic constants, bulk point defects, core properties of partial dislocation, and structure of disordered phases have already been performed with these potentials [7–9]. They conclude that, for each kind of system or physical mechanism, one must determine the best interatomic potential.

Recently, Godet *et al* [10] have studied the nucleation of dislocations from a surface step on silicon. The dislocation formation with this mechanism would explain the presence of dislocation observed in nano-materials [11] where the dimensions are too small to allow a classical multiplication mechanism like Franck–Read sources. This would also explain the appearance of dislocations from cleavage ledges, when silicon is plastically deformed at low temperature [12]. Since the observation of the very first stage of dislocation nucleation is difficult, the atomic simulation may bring up an interesting alternative. However, recently, Godet *et al* [13] have shown that the obtained results were potential dependent. During the process of nucleation of the dislocations, the atomic structure is so greatly deformed that the potentials go out of their usual domain of validity, which may explain these disagreements. It would be helpful to find out which is the silicon potential giving the best results in the case of large shears.

In this paper, an attempt is presented in view of determining the best interatomic potential for silicon subjected to large shear strain, by comparing results obtained for different potentials with *ab initio* calculations. First, considering homogeneous shear of bulk silicon, two criteria have been used for the potential selection. The first one bears upon the variation of the bulk energy as a function of the applied strain. The second criterion is related to atomic configurations in that it considers how imposed atomic displacements distribute between the shuffle and the glide sets of the {111} planes. In particular, we focus on the mechanism of atomic bonds switching from one neighbour to another. After the homogeneous shears, a second part is devoted to generalized stacking fault (GSF) energy surfaces, in particular their shape in both shuffle and glide set planes at large fault vectors. All these situations contribute to a better understanding of the strain properties of both glide and shuffle planes, related to the mechanisms of dislocations nucleation and mobility [14–17] or to the mechanisms of cleavage and fracture of this crystal [18–20].

2. Methodology

2.1. Shear techniques

In ambient conditions silicon crystallizes into the diamond cubic structure which is formed of two interpenetrating face centred cubic (fcc) sublattices called in the following sublattices 1 and 2. In this structure, the dislocations glide in the {111} dense planes with a $1/2\langle 110\rangle$ Burgers vector corresponding to the shortest vector of the fcc lattice. We have studied the silicon bulk under large shear strain, along the {111} planes in the $\langle 110\rangle$ direction, from zero

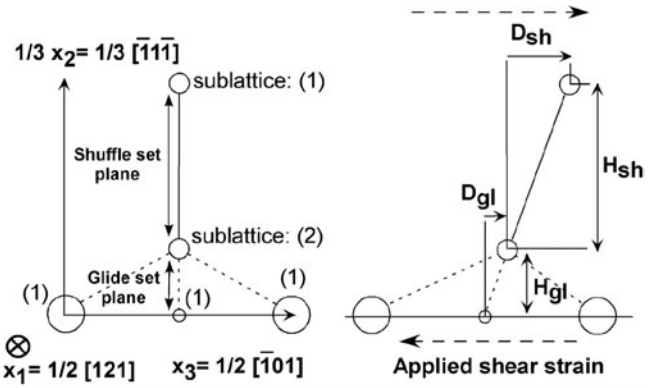

Figure 1. Definition of displacements and shear strains shown on a deformed structure (right) compared to the perfect lattice (left). In shuffle set planes the displacement is called $D_{\rm sh}$, and the shear strain is defined as $\frac{D_{\rm sh}}{H_{\rm sh}}$, $H_{\rm sh}$ being the 'height' of the shuffle set. In glide set planes, similar notations are taken.

up to a given shear strain, allowing us to recover the cubic diamond structure. As the cubic diamond structure includes two fcc sublattices, there are two kinds of {111} plane, that are alternately piled up, narrowly spaced between the (111) planes of the sublattices 1 and 2, and widely spaced between 2 and 1, called glide and shuffle set planes respectively [21] (figure 1). To deform the crystal, we have progressively applied shear strain increments of about 4% on both sublattices 1 and 2, up to a shear strain called $\gamma_{23\rm tot} \simeq 122\%$. This limit corresponds to the ratio of a slip in a shuffle set equal to a Burgers vector $\mathbf{b}$ ($=\mathbf{x}_3$) by the shuffle and glide set interplanar distance ($=\mathbf{x}_2/3$), i.e. $x_3/(x_2/3) = \sqrt{3}/\sqrt{2}$. After each shear increment, the atomic positions belonging to sublattice 2 are relaxed in all directions to minimize the energy. Note that the calculations are performed at 0 K and constant volume. The aim is to monitor the energy evolution during the shear, and determine how the homogeneous shear strain is divided between the shuffle set and the glide set. In this paper, we call displacement in one set (shuffle or glide) the shift after application of the strain (after relaxation), and shear strain in one set the ratio of the displacement by the interplanar distance in this set (figure 1). Note that interplanar distances may vary because sublattice 2 is free. However, as the shear is performed at constant volume, the addition of the shuffle and glide set interplanar distances remains constant. For the same reason, the bulk shear stress σ_{23} is obtained by the derivation of the atomic energy curve against the applied shear strain γ_{23}.

We have also calculated the GSF energy and the restoring forces along the slip directions in shuffle and glide planes. The unrelaxed GSF energy surface is obtained by simply moving one half of the crystal rigidly with respect to the other half along a cut plane in the middle of the crystal. The GSF energy is defined as a function of the relative displacement $\mathbf{f}$ of the two atomic planes immediately adjacent to the crystal cut plane. To calculate the GSF energy with atomic and volume relaxation, the atoms in the two planes immediately adjacent to the cut plane are restricted to move along the $\langle 111 \rangle$ direction only, in order to keep the relative displacement $\mathbf{f}$, whereas the other atoms relax in all directions. Therefore, the actual relative displacement $\mathbf{f}$ might be different from the displacement between the centres of both halves of the crystal. The restoring force in a given direction corresponds to the derivative of the GSF energy versus the displacement $\mathbf{f}$. Here, we focused on the $\langle 110 \rangle$ direction in the shuffle and glide set, and also on the $\langle 112 \rangle$ direction in the glide set, since perfect dislocations can be dissociated in two Shockley partial dislocations with $1/6\langle 112 \rangle$ Burgers vectors in that set.

The local shear stress required to maintain the displacement **f** in both sides of the cut plane is directly proportional to the opposite of the restoring forces.

2.2. Computational methods

First principles calculations of the bulk shear are performed using the ABINIT package [22], the exchange–correlation energy being determined within the local density approximation (DA) with the Teter Pade parametrization [23] which reproduces Perdew–Wang. The valence electron wavefunctions are expanded in a plane wave basis with a cut-off energy of 15 Hartree. The ionic potential is modelled by a norm conserving pseudo-potential from Troullier and Martins [24]. To simulate the bulk shearing process, a periodic cell orientated along $1/2[121](\mathbf{x}_1)$, $[\bar{1}1\bar{1}](\mathbf{x}_2)$ and $1/2[\bar{1}01](\mathbf{x}_3)$ is used, including 12 atoms, i.e. six {111} atomic planes (three glide set and three shuffle set planes) along $\mathbf{x}_2$. For the reciprocal space integration, we have used nine special k-points in the irreducible Brillouin zone when the cell is not sheared, and 15 special k-points when the cell is sheared owing to the reduced symmetry. The k-point lattice obtained with the Monkhorst and Pack scheme [25] is the reciprocal of the superlattice defined by the supercell in real space by $3\mathbf{x}_1$, $2\mathbf{x}_2$ and $5\mathbf{x}_3$, the origin of this k-point lattice being shifted by a [0.5, 0.5, 0.5] vector. The SCF cycle is stopped when the difference in total energy between two successive cycles is smaller than 10^{-10} Hartree. Metallic occupation of levels is allowed using the Fermi–Dirac smearing occupation scheme. The atomic positions are relaxed using the Broyden–Fletcher–Goldfarb–Shanno minimization down to forces smaller than 5×10^{-5} Hartree/bohr (2.5×10^{-3} eV Å^{-1}). We have compared our results with the *ab initio* study performed by Umeno and Kitamura [26] where the same calculation is realized with a full relaxation of volume and ionic position but only up to 35% of strain.

For the empirical bulk shear calculations, three different interatomic potentials have been used, Stillinger–Weber (SW) [27], Tersoff [28] and the environment-dependent interatomic potential (EDIP) [29]. The pioneering potential of SW has only eight parameters and is fitted to few experimental properties of both crystallized (cubic diamond) and liquid silicon. It consists of a linear combination of two- and three-body terms. The Tersoff functional form is fundamentally different from the SW form in that it includes many-body interactions thanks to a bond order term. As a result, the strength of individual bonds is affected by the presence of surrounding atoms. The final version called T3 has 11 adjustable parameters fitted to *ab initio* results for several Si polytypes. The third potential, EDIP, has a functional form similar to that of Tersoff but slightly more complicated. It incorporates several coordination-dependent functions to adapt the interactions for different coordinations. Thirteen parameters are determined by fitting to a fairly small *ab initio* database.

The dimensions of the calculation cell must be twice as large as the cut-off radius of the interatomic potentials to minimize interaction of atoms with their images in neighbouring cells. So a calculation cell with the same geometry as before is used, but containing 576 atoms. The relaxation of atomic positions is performed with a conjugate gradients algorithm until the magnitudes of the forces are smaller than 10^{-4} eV Å^{-1}.

The GSF energy surface calculations have been performed with the three interatomic potentials and we have compared our results with the GSF energy surfaces obtained with first principles calculations by Juan and Kaxiras [30, 31]. Note that several energy curves or unstable stacking fault energies have been calculated with those interatomic potentials [8, 32, 33]. Here, periodic conditions are applied only along the $\langle 112 \rangle$ and $\langle 110 \rangle$ directions. In the third direction, the number of {111} planes is large enough (30) to avoid spurious interactions between the free surfaces and the crystal cut plane. The system contains 1440 atoms.

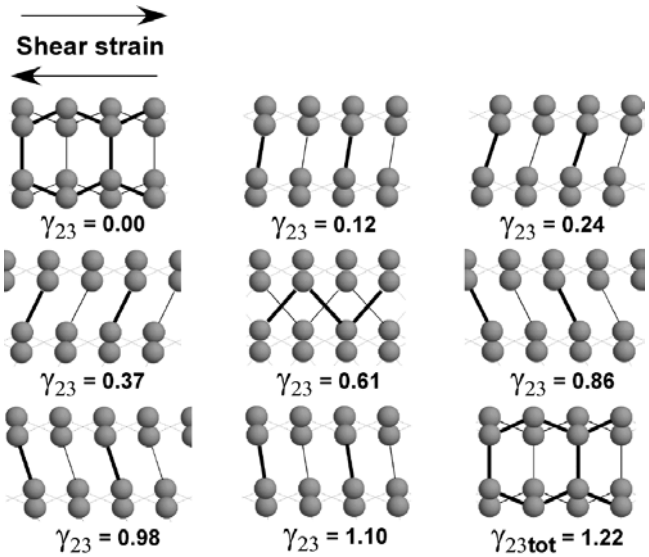

Figure 2. Snapshot of the bulk structure during homogeneous shear process. Here, bonds are drawn solely on the criterion of distance and are not indicative of true chemical bonds between atoms.

3. Results/discussion

3.1. Homogeneous shear strains

The calculation of homogeneous shear strain of bulk silicon has been performed *ab initio* and with the three interatomic potentials. The observation of the sheared atomic structure obtained with the *ab initio* calculation (figure 2) shows that the strains are essentially located in the shuffle set. The bonds between atoms across the shuffle set plane are successively weakened, broken and then formed again. This is confirmed by the monitoring of the electronic density where the covalent character of the bonds progressively vanishes to reach a metallic character at half of the applied shear strain in the shear direction ($\langle 110 \rangle$). Our calculation is in agreement with the *ab initio* study realized by Umeno and Kitamura [26], where it is found that the bandgap is progressively closed with the applied shear. At the maximum of the applied shear strain, each shuffle set plane has been shifted by a Burgers vector of a perfect dislocation and the diamond crystal is recovered.

To compare the different interatomic potentials, the atomic energy and the corresponding shear stresses as a function of the applied shear strain are calculated and represented in figure 3. For small strains, all the energy curves coincide and the stress curves are linear, indicating that the empirical potentials are fairly well fitted to the elastic coefficients. The shear modulus associated with $\langle 110 \rangle \{111\}$ shear at constant volume obtained from the *ab initio* calculation is around 52 GPa, close to the value calculated with volume relaxation [26] and also relatively close to the value obtained from the elastic coefficient calculated at 0 K ($C_{12} - \frac{1}{3}(2C_{44} + C_{12} - C_{11}) = 48.3$ GPa) [34]. For larger strains, the potentials may be classified into two groups depending on whether they are close or not to *ab initio*. SW belongs to the first group with energy curves in fair agreement with *ab initio* which presents smooth maxima of similar heights at half of the applied shear, whereas EDIP and Tersoff are in the other group with larger maxima and angle-shaped curves. Regarding stresses, the variations of

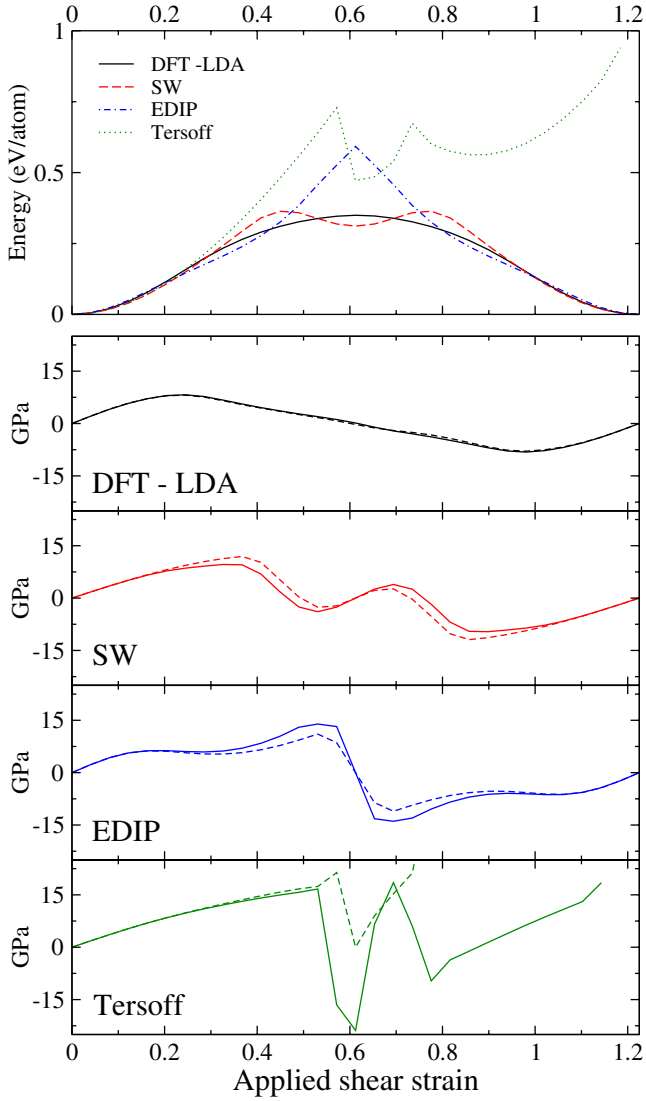

Figure 3. Upper graph: variation of atomic energy during the shear process (in eV/atom). Lower graphs: bulk shear stress σ_{23} in GPa (solid curve) and shear strain of the glide plane multiplied by a shear modulus in GPa (dashed curve), for the different potentials.

SW and *ab initio* are relatively smooth compared to EDIP and Tersoff, with similar theoretical shear strengths reached at about one-quarter of the total applied strain, while those obtained with EDIP and Tersoff are larger and reached at about half of the applied strain (table 1). Note that our *ab initio* theoretical shear strength at constant volume is relatively close to the value calculated with volume relaxation [26]. SW seems to be the best interatomic potential to model the shear stress evolution during the atomic bond switching. Probably the introduction of temperature would smooth the energy curves, and in the case of the Tersoff potential would allow the crossing of the energy barrier to recover the diamond crystal. However, the general shape of calculated curves will be preserved, in particular for deformations corresponding to theoretical shear strenghs.

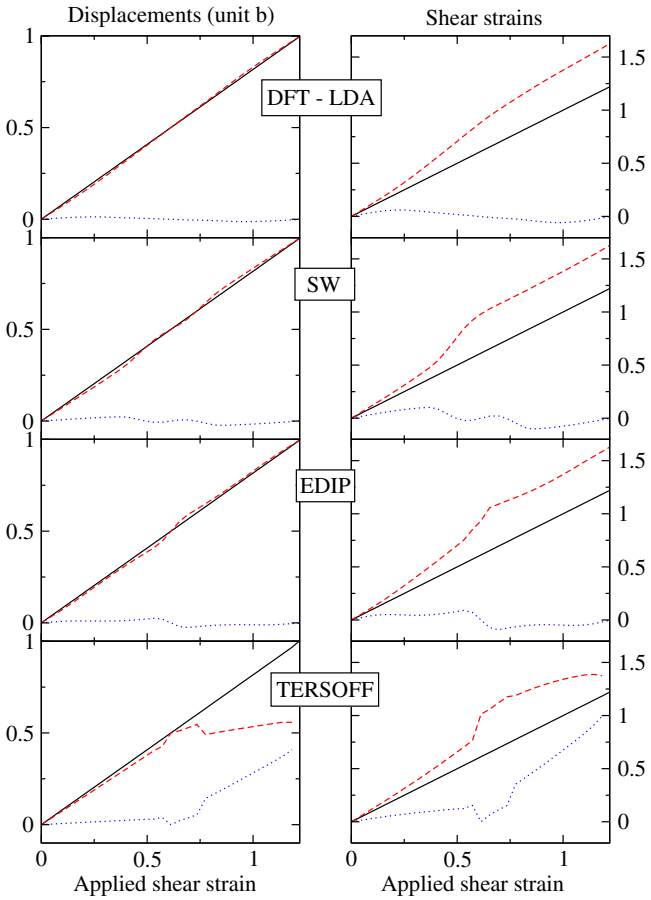

Figure 4. The left-hand panel shows the displacements in both shuffle (dashed curve) and glide (dotted curve) planes in unit *b* versus the applied shear strain. The solid line corresponds to the addition of shuffle and glide displacements. The right-hand panel shows the shear strain in both shuffle (dashed curve) and glide (dotted curve) planes versus the applied shear strain. The solid line corresponds to the applied strain.

Table 1. Theoretical shear strengths and strains obtained with different potentials.

	Constant volume				Volume relaxation
	SW	Tersoff	EDIP	DFT–LDA	DFT–LDA [26]
Theoretical shear strength (GPa)	9.6	16.7	13.9	7.95	10
Theoretical shear strain (%)	32.7	53	53	24.5	30
(% of the applied strain)	27	43	43	20	25

To analyse the atomic structure, the displacements and shear strains in both shuffle and glide set planes along the ⟨110⟩ shear directions have been determined (figure 4). For applied strains up to half the maximum, all potentials show a similar behaviour: the displacements in the shuffle set plane following the total displacement, while those in the glide set oscillate weakly with a magnitude lower than 0.15 Å. For larger applied strains, the displacements in

Table 2. Unstable stacking fault energies γ_{us} along relevant Burgers vectors (**b**), for the shuffle and glide planes in J m^{-2}, unrelaxed (U) and relaxed (R) with atomic and volume relaxation. (γ_{us} is not necessarily localized at $\mathbf{f} = b/2$.)

	SW		Tersoff		EDIP		DFT–LDA [31]	
	U	R	U	R	U	R	U	R
⟨110⟩ shuffle	1.38	0.83	2.57	1.50	2.16	1.32	1.84	1.67
⟨112⟩ glide	4.78	3.08	3.33	1.96	3.24	1.71	2.51	1.91
⟨110⟩ glide	26.09	6.21	31.19	5.27	13.43	6.14	24.71	≃5.55

the shuffle set reach the Burgers vector of a perfect dislocation. In the glide set they return to zero, except for the Tersoff potential where the displacements in the shuffle set remain practically constant and where the displacements are then located in the glide set along ⟨112⟩. The variations of shear strains in both planes show that the *ab initio*, SW and EDIP results are relatively close to each other. The interatomic potentials modelling these effects properly are SW and EDIP.

In figure 3, the shear strains of the glide set planes are represented with a dashed curve next to the bulk shear stress with a full curve. In all cases, while most of the displacements are localized in the shuffle set, the shear strains of the glide set are approximately linear with the bulk shear stresses, with a large shear modulus (μ), for example 134 GPa with *ab initio* calculations. The strains localized in the glide set then remain elastic and linear whereas those of the shuffle set do not. Moreover, the large shear modulus of the glide set shows that the displacements in the glide set, although always small, play an important role in the bulk shear stress. This is confirmed by the study of Umeno and Kitamura [26] where it is concluded that the subtle displacements in the glide set have a remarkable effect on the shear stress.

3.2. GSF energy and restoring force

We have investigated the GSF energy surfaces and the corresponding restoring forces in directions of Burgers vectors **b**, calculated with *ab initio* techniques [31] and interatomic potentials, in order to compare the localized shear stresses in the shuffle and glide set planes. Two directions have been investigated, ⟨110⟩ in the shuffle and glide set for perfect dislocations, and ⟨112⟩ in the glide set for Shockley partial dislocations.

Usually, one considers the maxima of the GSF energy, i.e. the unstable stacking fault energy γ_{us} (table 2), as an important parameter for gliding. In addition to γ_{us}, we also determine the maxima of the restoring force, τ_{max}, along the three directions (table 3). In all cases, the lowest values are obtained for the ⟨110⟩ direction in the shuffle set plane, as expected. The best γ_{us} are given by Tersoff and EDIP, the SW potential tending to underestimate in the shuffle set and to overestimate in the glide set. Regarding the restoring force, the SW potential yields the best results, the large values for EDIP and Tersoff coming from the singularities in the curves. It appears that the sole determination of these maxima is not enough to discriminate between the potentials. An additional indication is given by the location of the maxima. The best agreement with *ab initio* is then obtained for the SW potential, with maxima in the vicinity of 0.3 b, whereas for both EDIP and Tersoff they are located at displacements greater than 0.4 b.

Instead of only considering maxima, we compared directly the variations. Along the three directions, the *ab initio* GSF energy variations, calculated by Juan and Kaxiras [31], are smooth, with sinusoidal-shaped curves. Comparing with the GSF energy for the three potentials (figure 5), the best qualitative agreement is obtained with the SW potential. Both EDIP and

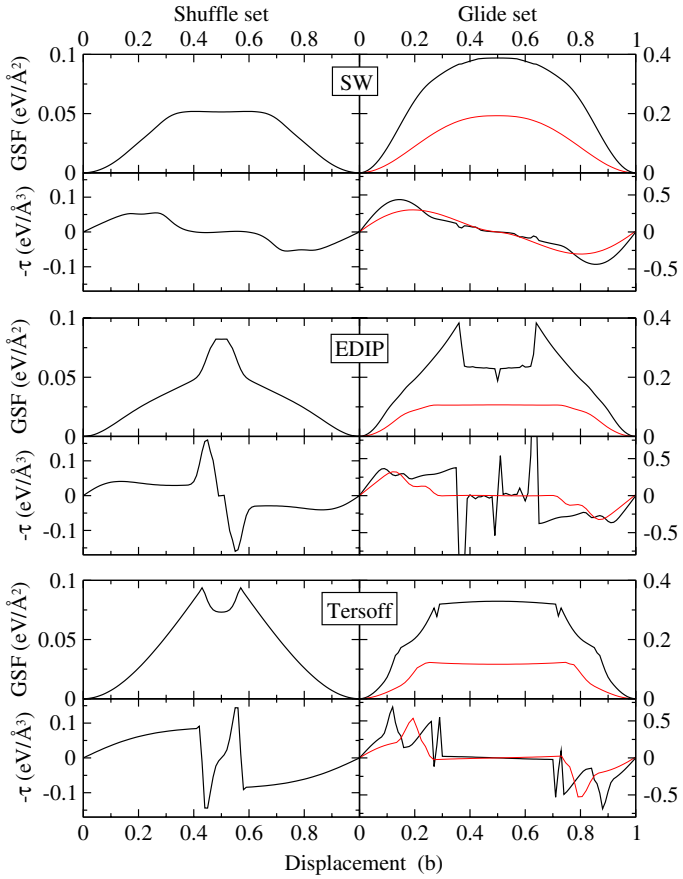

Figure 5. The fully relaxed GSF energies and the corresponding restoring force $(-\tau)$ on the shuffle (left) and glide (right) set planes (bold curves for ⟨110⟩ and thin curves for ⟨112⟩ directions) for the three interatomic potentials.

Table 3. Maximum value of the restoring force τ_{max} for the relevant directions (in eV Å^{-3}).

	SW	Tersoff	EDIP	DFT–LDA [31]
⟨110⟩ shuffle	0.055	0.144	0.160	0.093
⟨112⟩ glide	0.299	0.535	0.322	0.174
⟨110⟩ glide	0.437	0.688	1.908	0.268

Tersoff show large and abrupt variations of the GSF energy, as soon as the displacement is greater than 0.4 b. In particular, distorted shapes and angular points are present for EDIP in the glide set, and Tersoff in the shuffle set. If we focus on the favoured glide direction for perfect dislocation, i.e. the ⟨110⟩ in the shuffle set plane, it appears that the Tersoff potential shows the worst results, with a deep local minimum at 0.5 b. Using EDIP and SW, instead, leads to an energy maximum at 0.5 b, as obtained with the *ab initio* calculation. The whole EDIP and SW GSF energy curves are in fair agreement with *ab initio*, although the smoothest variations are obtained with SW.

More indications can be gained from the calculation of the restoring forces in the three cases. The variations, represented in figure 5, are similar to the bulk shear stress curves, shown

in figure 3. The various conclusions drawn from the analysis of the GSF energy variations remain valid here. The best agreement is obtained for the SW potential, with a rather smooth variation of the restoring force in all directions. With EDIP, discontinuous variations are obtained for displacements along ⟨110⟩ in both glide and shuffle sets. In particular, the restoring force along the favoured direction, ⟨110⟩ in the shuffle set, increases to a large maximum just before 0.5 b, and then suddenly drops to a symmetric minimum. This sharp behaviour is not observed in the *ab initio* curve. The last potential, Tersoff, shows the worst results, with discontinuities between 0.4 b and 0.6 b in the shuffle set, so in the range of large deformation, but also for small displacements in the glide set.

4. Conclusion

We have investigated the properties of bulk silicon subjected to a homogeneous shear, using *ab initio* techniques. It appeared that the shear takes place almost entirely in the shuffle set planes, with only slight displacements in the glide set planes. The atomic bonds between atoms on both sides of the shuffle set progressively lose their covalent character until a metallic state is established in the shear direction at half the maximum applied shear. Then the reverse process is observed, and the perfect diamond crystal structure is recovered. We have shown that glide set plays a predominant role in the bulk shear stress and that the strains localized in the glide set are linear and elastic with respect to the bulk shear stresses, with a large shear modulus. At 0 K, silicon can be viewed as formed by a stacking of 'elastic' glide set planes and 'plastic' shuffle set planes. Our results are confirmed by the analysis of GSF energy surfaces and restoring forces, determined with *ab initio* calculation [31], which suggests that the shuffle set is the favoured place for the glide event at 0 K. The variations of bulk shear stress are similar to the variations of the restoring force in the active glide plane. So at 0 K, a correct description of the restoring force is a prerequisite to model glide events.

One of the main objectives of this work was the determination of the best interatomic potentials in the case of greatly deformed silicon systems. We have then performed calculations of sheared bulk silicon and GSF energy surfaces with SW, Tersoff and EDIP potentials, and compared with *ab initio* results. For sheared bulk silicon we observed that EDIP and SW provided a faithful description of the glide event, and strain and stress analysis showed that the theoretical shear strength is better determined with SW. Regarding the GSF energy surfaces and restoring forces, it appears that the shuffle set is the preferred place for the glide events at 0 K for all the potentials, but the best value of the restoring force (τ_{max}) is given by SW. It must also be emphasized that the smoothest description of the glide of one plane on another is also obtained with SW. In summary, under large strains, SW seems to be the best potential to model qualitatively silicon.

This work was partially motivated by a previous work on the dislocation nucleation process from a surface step under a uniaxial stress [10]. In fact, in that case, a large homogeneous shear strain is present in the atomic structure. Our results explain why it is possible to model the nucleation process with the SW potential, whereas a potential like Tersoff leads to fracture or local amorphization under stress.

Finally, one possible explanation for the differences between the potentials, such as the discontinuities and local minima on the energy and stress, may come from the cut-off radius of each potential. In fact, when the atomic structure is greatly deformed, the number of atoms taken into account in the energy calculation may abruptly change, leading to sharp energy variation. The smooth behaviour of SW may then be explained by its relatively large cut-off radius of 3.77 Å. Another possible explanation is the simplicity of its functional form and the small number of fitted parameters. For Tersoff and EDIP, the functional is more complicated

with more parameters. While this is required to model properly a large range of experimental quantities, a more complex functional may lead to non-physical behaviours, when the atomic structure is far from the equilibrium state.

References

[1] Öberg S, Sitch P K, Jones R and Heggie M I 1995 *Phys. Rev.* B **51** 13138
[2] Justo J F, Fazzio A and Antonelli A 2000 *J. Phys.: Condens. Matter* **12** 10039
[3] Ewels C P, Wilson N T, Heggie M I, Jones R and Briddon P R 2001 *J. Phys.: Condens. Matter* **13** 8965
[4] Justo J F, Antonelli A and Fazzio A 2001 *Solid State Commun.* **118** 651
[5] Pizzagalli L, Beauchamp P and Rabier J 2003 *Phil. Mag.* **83** 1191
[6] Rasmussen T, Vegge T, Leffers T, Pedersen O B and Jacobsen K W 2000 *Phil. Mag.* A **80** 1273
[7] Balamane H, Halicioglu T and Tiller W A 1992 *Phys. Rev.* B **46** 2250
[8] Justo J F, Bazant M Z, Kaxiras E, Bulatov V V and Yip S 1998 *Phys. Rev.* B **58** 2539
[9] Moriguchi K and Shintani A 1998 *Japan. J. Appl. Phys.* **37** 414
[10] Godet J, Pizzagalli J, Brochard S and Beauchamp P 2002 *Scr. Mater.* **47** 481
[11] Wu R X and Weatherly G C 2001 *Phil. Mag.* A **81** 1489
[12] Argon A S and Gally B J 2001 *Superlatt. Microstruct.* **45** 1287
[13] Godet J, Pizzagalli L, Brochard B and Beauchamp P 2003 at press
[14] Duesbery M S and Joós B 1996 *Phil. Mag. Lett.* **74** 253
[15] Justo J F, Antonelli A and Fazzio A 2001 *Physica* B **302/303** 398
[16] Bulatov V V, Justo J F, Cai W, Yip S, Argon A S, Lenosky T, de Koning M and Diaz de la Rubia T 2001 *Phil. Mag.* A **81** 1257
[17] Rabier J, Cordier P, Demenet J L and Garem H 2001 *Mater. Sci. Eng.* A **309/310** 74
[18] Pérez R and Gumbsch P 2000 *Acta Mater.* **48** 4517
[19] Gally B J and Argon A S 2001 *Phil. Mag.* A **81** 699
[20] Pirouz P, Demenet J L and Hong M H 2001 *Phil. Mag.* A **81** 1207
[21] Hirth J P and Lothe J 1982 *Theory of Dislocations* (New York: Wiley)
[22] The ABINIT code is a common project of the Université Catholique de Louvain, Corning Incorporated and other contributors (http://www.abinit.org)
[23] Goedecker S, Teter M and Huetter J 1996 *Phys. Rev.* B **54** 1703
[24] Troullier N and Martins J L 1991 *Phys. Rev.* B **43** 1993
[25] Monkhorst H J and Pack J D 1976 *Phys. Rev.* B **13** 5188
[26] Umeno Y and Kitamura T 2002 *Mater. Sci. Eng.* B **88** 79
[27] Stillinger F H and Weber T A 1985 *Phys. Rev.* B **31** 5262
[28] Tersoff J 1989 *Phys. Rev.* B **39** 5566
[29] Bazant M Z, Kaxiras E and Justo J F 1997 *Phys. Rev.* B **56** 8542
[30] Kaxiras E and Duesbery M S 1993 *Phys. Rev. Lett.* **70** 3752
[31] Juan Y M and Kaxiras E 1996 *Phil. Mag.* A **74** 1367
[32] Duesbery M S, Michel D J, Kaxiras E and Joos B 1991 *MRS Symp. Proc.* **209** 125
[33] de Koning M, Antonelli A, Bazant M Z and Kaxiras E 1998 *Phys. Rev.* B **58** 12555
[34] Karki B B, Ackland G J and Crain J 1997 *J. Phys.: Condens. Matter* **9** 8579